Comprehensive Analysis and Configuration of a Control Loading Solution for a Rotary Wing Flight Simulator

Marco Rinaldi
Ph.D. Student
Politecnico di Torino
Torino, Italy

Pierluigi Capone
Lecturer
ZHAW
Winterthur, Switzerland

Giorgio Guglieri
Full Professor
Politecnico di Torino
Torino, Italy

ABSTRACT

This paper presents the design methodologies of a Control Loading System (CLS) drive model for the Research and Didactics Simulator (ReDSim) of the Zurich University of Applied Sciences (ZHAW). The analysis of the CLS hardware and interface software is presented. The CLS drive model is intended as an irreversible flight control system of a rotary wing aircraft's collective control, with trim system and force feedback capabilities, mainly as a function of the lever's position. The CLS motor's control parameters are set to fit the application's performance requirements. The drive model is developed in MATLAB/Simulink and is integrated with the XV-15 tiltrotor model of the ReDSim. Two different system identification techniques, the Least Squares and a convex relaxation-based Set-Membership approach, are used to estimate the parameters of the CLS hardware and consequently assess its fidelity to a model of reference. The implementation in the ReDSim has been rated by the pilot according to the Cooper-Harper handling qualities rating scale.

INTRODUCTION

Flight simulators' utility has come to an extent such that they are a necessary tool for all aviation training programs all over the world. The saving of money and resources, the safe environment for the pilot's training to both standard and potentially dangerous flight procedures, the negligible direct environmental impact with respect to real aircraft represent the main advantages of flight simulators. Flight simulators have also been under the study of the aerospace and engineering research world for more than 70 years, with the main focus of improving their fidelity to the real aircraft systems of interest. The Zurich University of Applied Sciences (ZHAW) offers a research real-time flight simulator (ReDSim) that can simulate both fixed and rotary wing aircraft such as jets, helicopters, gliders, tiltrotor aircraft thanks to the reconfigurable cockpit environment. During the simulation acoustic, visual and force feedbacks are given to the pilot by the sound generator, the visual computation system that displays a 180° view and a Control Loading System (CLS) attached to the controls. The simulator is driven directly by MATLAB/Simulink models. According to references [1],[2],[3],[4],[5] modern control loading systems are digitally controlled loaders that replicate the force feedbacks of the actual aircraft control hardware to be simulated. The cockpit's controls are rigidly attached to the load cell. Load cell actuation systems rely on two main control loops: the force loop, or outer loop, and the inner loop. The force loop is a model follower and computes the target position of the stick from the difference between the loader force and the target feedback force, applied to a model mass.

The inner loop is the motor control and exploits the outer loop's target velocity and position to generate the actuator's drive signal. As a consequence, the pilot applied force is given by the load cell force and the stick follows the model mass behavior. This paper illustrates the comprehensive analysis, design and validation of a pilot-oriented control loading solution for simulating the collective pitch control of a tiltrotor aircraft, whose model is already been implemented in the ReDSim by the previous work of reference [6], and later improved with the novel gimballed rotors model of reference [7]. The proposed Control Loading Solution is independent on the CLS connected to the other cockpit controls of the ReDSim: the collective control is located in the cockpit when a rotary wing aircraft model is used for simulation.

ANALYSIS AND SIMULATION OF THE EXPERIMENTAL SYSTEM

The adopted CLS hardware is purchased from an external company. A collective lever with a helicopter joystick controller on top of the grip is mounted on the axis hinge of the CLS hardware, shown in Figure 1.

Figure 1. Collective lever mounted on the CLS hardware

On the basis of the information provided by the CLS interface software, a generalized simulation model of the CLS control loops is developed in MATLAB/Simulink, as showed in Figure 2 and Figure 3.

The control logic is decoupled in two parts: the outer loop and the inner loop. The outer loop generates the reference velocity and position signals for the inner loop, as a model follower: the force error between the loader's torque and the reference force feedback is applied to a reference mass. The inner loop contains the motor control: the reference position and velocity are compared to their corresponding measurements, an anti wind-up proportional integral (PI) controller generates the command torque for the motor, which is a Permanent Magnet Synchronous Motor (PMSM) subjected to Field Oriented Control (FOC). According to reference from [8] to [10], FOC is one the most effective control techniques for PMSMs, as it based on the transformation of three-phase time varying stator's currents and voltages into two-phase stationary quantities by means of transformation matrixes, Park and Clarke transformations, that express the relation among the stator's fixed reference frame and the rotor's direct and quadrature reference frame, which is rotating with the rotor itself. The motor's current control action is implemented by means of two anti wind-up PI controllers: the direct current component is forced to zero to maximize the rotor's quadrature current, which is directly proportional to the motor's generated torque. The direct and quadrature current components are the motor current components expressed in the rotor's reference frame. The stator current components are expressed in a stationary stator's reference frame. The rotor's position has to be known at each sampling instant in order to derive the relative inclination of the stator and rotor's reference frame. Reference [11] presents the theoretical foundations of PID control and is used as a baseline for the control parameters tuning. Figure 4 shows the simulation results with a step pilot force.
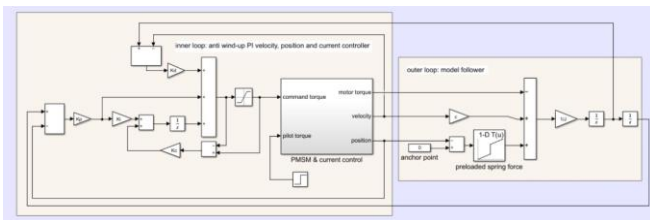

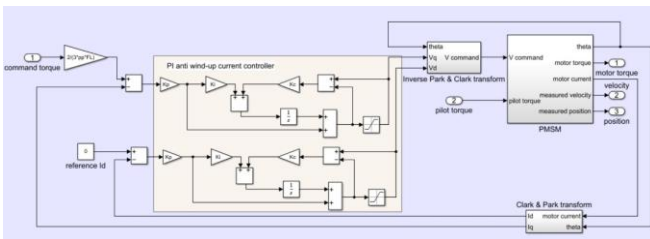**Figure 2. CLS outer and inner loop Simulink model**

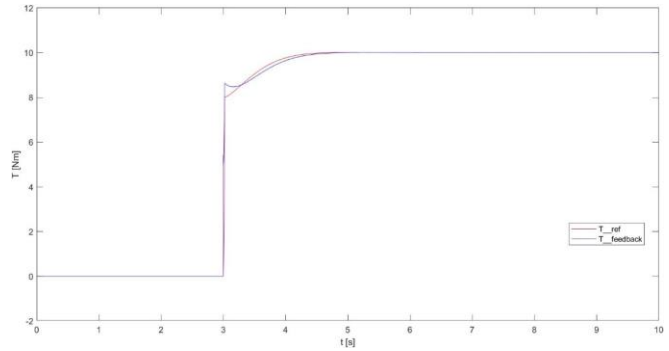**Figure 3. *PMSM & current control* subsystem**

Figure 4. Reference motor's feedback torque (red) and generated motor toque (blue) from a pilot step input force

Such a simulation model of the CLS hardware control logic is needed since the system's behavior of force feedback release, tracking of position commands and axis stability, depend on the motor's control parameters which can be set from an interface software.

## CONTROL LOADING SYSTEM DRIVE MODEL DESIGN

The purpose of the work is the development of a CLS drive model that implements the main functionalities of an irreversible collective control of a rotary wing aircraft, which are provided by the trim system connected to the collective axis. A fly-by-wire collective trim unit is considered, consisting of the following main elements:

- Preloaded spring: is in between two drive plates, holds the lever in the anchor position, i.e., trim position, provides controllability to the control itself through force feedback proportional to the displacement about the anchor point and a detent action for small movements about the anchor point. The feedback force profile is a function of the lever's position with respect to the anchor point: it's the sum of the contributions of preload, spring stiffness, damping and friction units.
- Damping unit: provides a smooth return to the anchor point.
- Friction unit: provides a backup for the damping unit and helps the spring in holding the lever in the anchor position.
- Trim Button (TB): until pressed, sends commands to an electric motor to move an irreversible gearbox and consequently the anchor point in both directions, with no force feedback for the pilot.
- Force Trim Release button (FTR): until pressed, the clutch is open, the pilot moves the anchor point and set it to the position corresponding to the button's release instant. The FTR is a spring-like button and comes back to its anchor point if released. The

feedback force is given by damping and friction units.

- Permanent force Trim Release button (PTR): doesn't need to be kept pressed for the FTR functionality.

A schematic representation of a collective trim unit main components is shown in Figure 5.
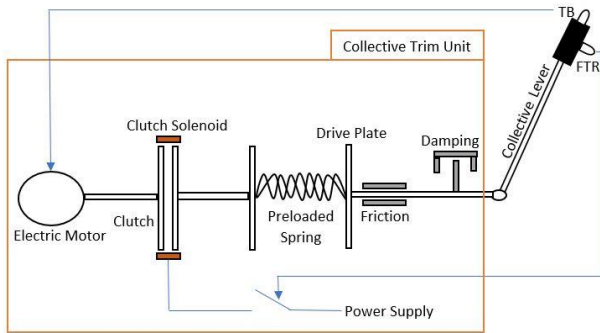
Figure 5. Schematic representation of a collective trim unit

Software design

The CLS drive model is developed in MATLAB/Simulink for consistency with the ReDSim's software environment, which is also MATLAB-based. The CLS hardware is connected to the simulation software via remote control, since MATLAB is not a directly supported. The data between the unsupported software and the CLS hardware are exchanged through TCP/UDP protocols. A MATLAB S-function written in C++ at the Centre for Aviation of ZHAW links the CLS hardware and the drive model, ensuring also the real-time execution of the model. The S-function is a MATLAB function that allows to integrate and run a source code, compiled as a Mex file, together with a Simulink model. The S-function, at each sampling instant of the drive model, outputs the measured CLS force and position, receives as inputs from the CLS drive model the hardware's settings of friction and damping, the scale factor of the force profile in percentage as well as directional force and position commands. The S-function inputs are the CLS drive parameters. A MATLAB initialization file sets the S-function parameters that are the constant settings of the CLS hardware throughout the whole simulation: force profile, axis travel and machine IP. The block diagram schematics of the software design is reported in Figure 6.
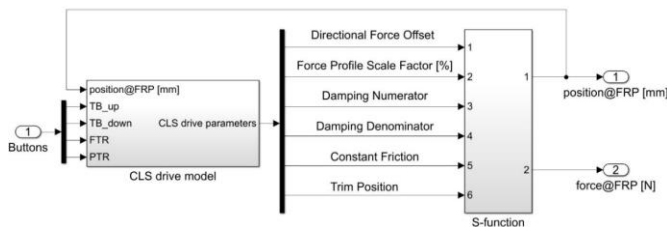
Figure 6. Block diagram overview of the software components

Inputs and outputs of the S-function are in the CLS hardware's own measurement units. The force applied on the collective axis is measured at the hinge of the axis itself, the axis position is measured at the hinge by a linear incremental encoder. *Constant Friction* is a parameter directly proportional to the internal friction of the CLS hardware, the internal damping is inversely proportional to the ratio between *Damping Numerator* and *Damping Denominator*. Force and position gearing factors convert the CLS hardware measurements at the hinge into measurements of position and pilot's applied force at the finger reference point (*FRP*) of the grip mounted on the collective axis. The force measurement of reference *force@FRP* is the force applied perpendicularly to the lever's grip at the *FRP*. The position measurement of reference *position@FRP* is the linear displacement of the *FRP* from the axis central position projected onto the direction of the force measurement of reference. With such a gearing among the CLS hardware's measurements and the converted *FRP*-related measurements, all the samples refer to the same point and to a mutually equal direction of motion. As illustrated in Figure 7, the true *FRP* motion is along the circumference with radius r centered at the hinge H, the direction of the linear approximation of motion $d1$ is projected onto the direction $d2$, which is perpendicular to the lever and is the same direction of the pilot applied force at the *FRP*. β is computed from basic geometrical calculations derived from the lever's technical designs. The force gearing factor is derived exploiting a dynamometer. The implementation of the gearing factors is realized by means of mono-dimensional look-up tables with linear interpolation from the breakpoints. For the sake of clarity, it is reported that an upward *FRP* motion and a pulling pilot force are considered with positive sign.
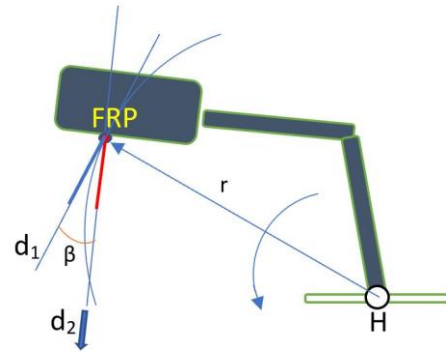
Figure 7. Schematic representation of the *FRP* direction of motion and pilot applied force

The simulated CLS hardware control loops refer to a "force feedback" mode, therefore the capability of the system to follow position commands depends on the force curve. The motor's control parameters are set from the interface software

in order to have a stable axis with respect to the selected damping parameter and a smooth position tracking.

Experimental set-up and parameters estimation

The system is modelled as an equivalent linear mass-spring-damper system, which is consistent with respect to the control hardware of the collective unit of reference, shown in Figure 5. (1) shows the continuous time transfer function of the system, where c is the damping coefficient, k is the spring stiffness and m is the equivalent mass at the *FRP*:

$$G(s) = \frac{X(s)}{F(s)} = \frac{1}{m*s^2+c*s+k} \tag{1}$$

The equivalent mass of the lever at the *FRP* is a non-linear function of the *FRP* position. The gravity profile of the *FRP*, as a function of the position, is derived as the linear piece-wise approximation of two non-linear gravity profiles. As shown in Figure 8, the CLS hardware is given ramp trim commands from one axis travel limit position to the other in both directions, sampling the *FRP* force.
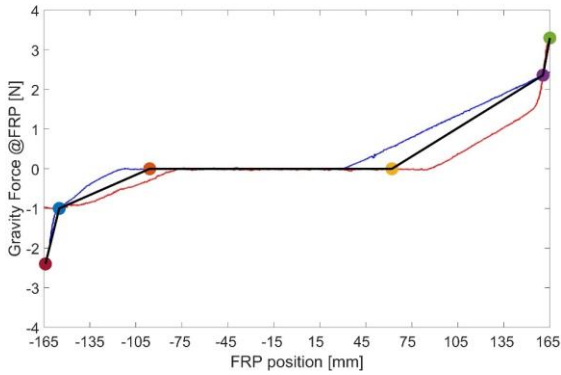

Figure 8. Gravity profile at the *FRP*

The gravity profile is subtracted to the estimation data set of friction and damping coefficients, taken with null force profile and different CLS damping and friction parameters. Damping and friction can be set and estimated independently: each of the parameters is set to the lowest value during the data collection for the other one's estimation and the movement of the collective during the data collection makes the force contribution of the estimated parameter massively prevailing with respect to the other parameter contribution. The classical LS estimator, for which reference [12] is considered the baseline, is used as identification method since the model is static and number of experimental data is high. This makes the LS estimator a robust choice. The estimation model is presented in (2):

$$F(k) = c * v(k) + F_d * sign(v(k)) + e(k) \tag{2}$$

where k is the sampling instant, F_d is the dynamic friction coefficient, F is the measured *FRP* force, v is the *FRP* derived

velocity, e is the additive random noise. Figures 9,10 show the dataset setup for damping and friction coefficients estimation. The estimation results are shown in Figures 11,12.
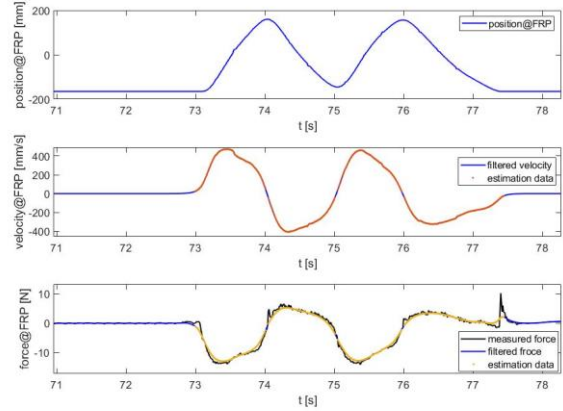

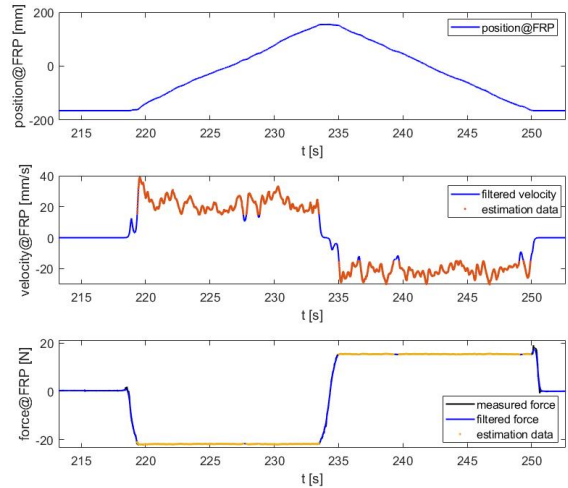**Figure 9. Dataset for damping estimation, extracted from a simulation**

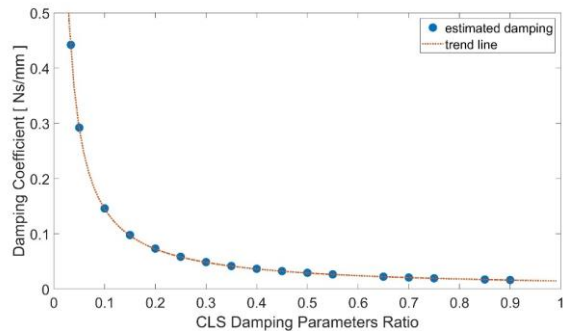**Figure 10. Dataset for friction estimation, extracted from a simulation**
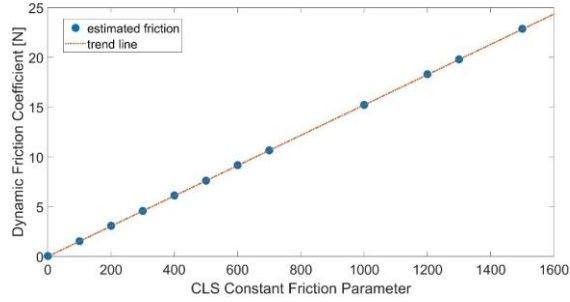

Figure 11. Damping estimation results

Figure 12. Friction estimation results

In the LS formulation of (2) a unique damping parameter is imposed for friction estimation and vice versa to stress the decoupling. The estimation results are confirmed with acceptable variation if another measuring instrument is used. In particular, a 3-Axis Linear Accelerometer is rigidly connected to the lever of the CLS hardware at the *FRP* location. Only the z-axis acceleration component is considered for data acquisition as it is along the d_2 direction of Figure 7. The data are processed a median filter to suppress the noise, assumed to be random, while preserving the signal' peaks and a low pass filter to smooth the signal, as shown in Figure 13.
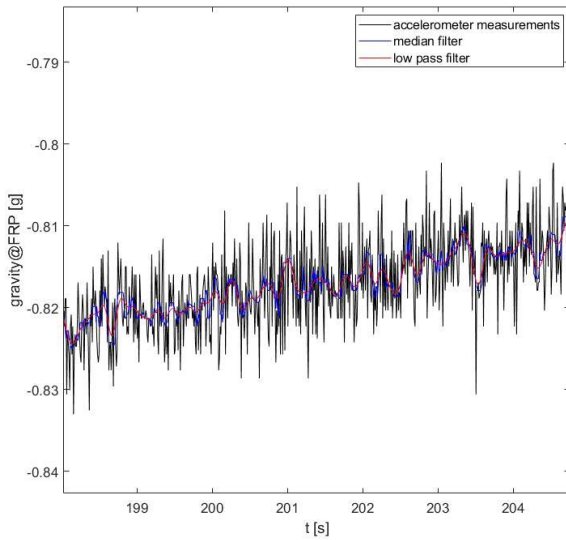
Figure 13. Accelerometer's signal processing in time domain

The data are synchronized with the CLS hardware force and position measurements. The gravity acceleration component on the z-axis is characterized as a function of the *FRP* position and it's subtracted from the measured acceleration in correspondence of each *FRP* position, as shown in Figure 14.
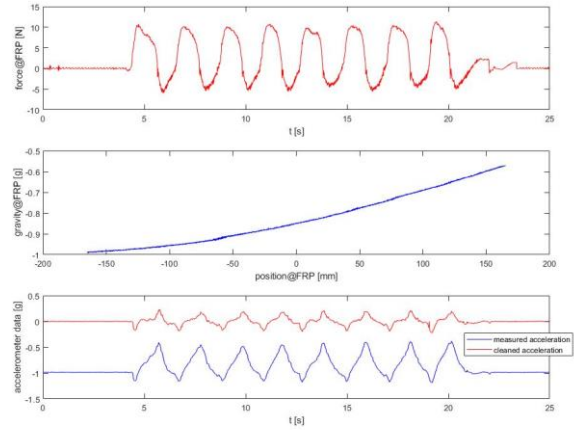
Figure 14. Synchronization with CLS measures, gravity profile at the *FRP* and accelerometer data, extracted from a simulation

The estimation of damping and dynamic friction coefficients by means of the LS method is repeated exploiting the velocity data integrated from z-axis acceleration data. The discrepancy between the parameters estimated with a combination of accelerometer and CLS measurements and with CLS measurements-only is of at most 10%. Such a discrepancy is acceptable considering that the sensor's calibration is basic. The experimental data extracted from a simulation in which the lever is repetitively moved in both directions along the full travel are shown instead. The upper part of Figure 15 shows the velocity signal derived from the CLS measured position (blue) and the integrated accelerometer's clean data (red), with a trapezoidal cumulative integral function. The lower part of Figure 15 shows the CLS measured force at the *FRP* (blue) and the force signal reconstructed with the accelerometer-derived velocity (red) and the estimated parameters.
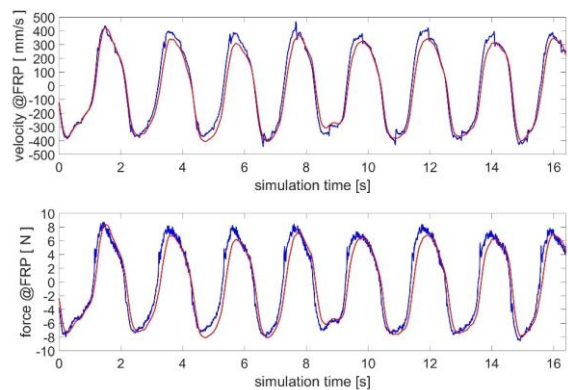
Figure 15. Comparison between accelerometer data and CLS hardware data, extracted from a simulation

The effectiveness and ease of replicability of the proposed characterization of the control loading solution is confirmed by the estimation results obtained with the accelerometer data.

Such a characterization, despite being constrained to the approximated *FRP* linear motion and *FRP* pilot force, can easily find experimental validation, independently on the lever's shape and sensors' location.

It is worth noticing that the consistency property of the classical LS estimator holds for static models with output-error noise structure and if the data are corrupted by an identically distributed random noise with zero mean value and gaussian distribution. In the LS problem formulation, the input data are also corrupted by noise. In order to give stronger theoretical foundations and validate the results, considering the approach of estimating the parameters of a discrete time linear time invariant system with error-in-variable noise structure discussed in reference [13], the problem is formulated as a nonconvex polynomial optimization problem. The process transfer function (1) is discretized with the Forward Euler method and is showed in (3) and (4), where T_s is the sampling time.

$$G(z) = \frac{X(z)}{F(z)} = \frac{\theta_3 * z^{-2}}{1 + \theta_1 * z^{-1} + \theta_2 * z^{-2}} \ , \tag{3}$$

$$\theta_1 = -2 + \frac{T_s * c}{m}, \ \theta_2 = 1 + \frac{T_s^2 * k - T_s * c}{m}, \ \theta_3 = \frac{T_s^2}{m} \tag{4}$$

The feasible parameter set D_θ shown in (5) is defined by the process transfer function (3) expressed in regression form and the noise that corrupts the measured position and force X_M, F_M. The input and output noise variables ε and η are assumed to be bounded by E and N, respectively. $D_{\theta,\eta,\varepsilon}$ shown in (6) is the reformulation of (5) in an higher dimensional space with noise variables taken explicitly into account in the parameter set formulation, with N_s number of samples.

$$D_\theta = \{\theta \in R^3 :$$

$X(k) + \theta_1 * X(k-1) + \theta_2 * X(k-2) = \theta_3 * F(k-2),$
$with \ k = 3, \dots, N_s \ ;$
$X(k) = X_M(k) - \eta(k) \ ,$
$F(k) = F_M(k) - \varepsilon(k) \ ,$
$|\varepsilon(k)| \leq E \ ,$
$|\eta(k)| \leq N \ ,$
$with \ k = 1, \dots, N_s \} \tag{5}$

$$D_{\theta,\eta,\varepsilon} = \{\theta \in R^3, \eta \in R^{N_s}, \varepsilon \in R^{N_s} \ :$$

$X_M(k) + \theta_1 * X_M(k-1) + \theta_2 * X_M(k-2) - \eta(k) - \theta_1 * \eta(k-1) - \theta_2 * \eta(k-2) = \theta_3 * F_M(k-2) - \theta_3 * \varepsilon(k-2) \ ,$
$with \ k = 3, \dots, N_s \ ;$
$|\varepsilon(k)| \leq E \ ,$
$|\eta(k)| \leq N \ ,$
$with \ k = 1, \dots, N_s \} \tag{6}$

For every parameter θ belonging to $D_{\theta,\eta,\varepsilon}$, (6) can be formulated as an optimization problem with polynomial constraints given by the regression form of (3) and the noise bounds, as showed in (7).

$$PUI_\theta = [\theta_{min}, \theta_{max}]$$

$$\theta_{min} = min_{\theta,\eta,\varepsilon}(\theta) \ ; \ \theta_{max} = max_{\theta,\eta,\varepsilon}(\theta)$$

subject to:

- $X_M(k) + \theta_1 * X_M(k-1) + \theta_2 * X_M(k-2) - \eta(k) - \theta_1 * \eta(k-1) - \theta_2 * \eta(k-2) = \theta_3 * F_M(k-2) - \theta_3 * \varepsilon(k-2)$
- $\varepsilon(k) \leq E$
- $\eta(k) \leq N$
- $\varepsilon(k) \geq -E$
- $\eta(k) \geq -N \tag{7}$

A convex relaxation technique based on Linear-Matrix-Inequalities (LMI) constraints is used to solve the original non-convex problem and compute the parameters uncertainty intervals (PUI) which are defined by the maximum and minimum parameters bounds. The relaxation method is implemented by the sparsePOP Matlab software. The adopted set-membership identification method provides theoretical foundations to the results obtained with the classical LS estimator, but requires higher computational effort, longer run times and leads to similar results as far as the central estimate is concerned. As showed in Table 1, the parameters estimated with the LS method are inside the relaxed bounds. The inertial contribution is negligible, as the data are taken from the "zero *FRP* gravity" position range of Figure 8.

Table 1. Comparison of LS and set-membership estimated parameters

	CLS setting	LS	min	max
M [Ns²/mm]	/	/	0.0834	0.132
	/	/	0.0859	0.127
	/	/	0.0901	0.119
	/	/	0.0761	0.107
c [Ns/mm]	0.033	0.442	0.354	0.489
	0.1	0.146	0.09	0.152
	0.2	0.0732	0.0568	0.0805
	0.3	0.0488	0.0421	0.0698
k [N/mm]	0.17	/	0.148	0.184
	0.17	/	0.163	0.191
	0.17	/	0.157	0.182
	0.17	/	0.162	0.190

CLS drive model

The CLS drive model is developed in MATLAB/Simulink and is integrated with the XV-15 tiltrotor aircraft model of the ReDSim.

The Simulink model that drives the CLS hardware is shown in Figure 16, its subsystem *set trim point* is shown in Figure 17. The inputs of the CLS drive model are the buttons *FTR*, *PTR*, TB toward both directions *TB_up*, *TB_down* and the measured position at the *FRP position@FRP*. The red colored CLS drive model components belong to the Boolean domain. All the switches in the model are defined such that if the

second input is true, the first input is passed, otherwise the third input is passed.

From the start of the simulation, the CLS hardware initializes, moving towards the simulation's initial trim position. A binary parameter (BP) enables the CLS hardware to come back to the trim position. The S-function sets BP to 0 for the first two sampling instants of the simulation time. At the second sampling instant the trim position is equal to the measured position at the first sampling instant, BP is set to 1, the axis moves at a rate of 100mm/s towards the initial trim position *starting trim*. The initialization brings to a smooth initialization of the collective independently on the final position of the previous simulation and the initial value of the unit delay. This is due to the fact that, as soon as the CLS hardware is enabled to come back to the anchor point, its measured position and its trim position coincide. It is not possible to impose the first trim position command coincident with the first measured position, because of algebraic loops.

If the pilot operates the collective without pressing any button, the CLS hardware acts like a spring according to the defined force profile. The force profile defines the spring contribution to the total feedback force. Three spring force profiles are defined, as reported in Table 2.

Table 2. Spring Force Profiles Characteristics.

Profile	Preload [N]	Gradient [N/mm]	Max Travel [mm]
Fly-by-Wire	8	0.17	100
NextGen	8	0.34	50
Classic	8	0.085	240

Pressing either *FTR* or *PTR* has the same effect: *Force Profile Scale Factor* is set to 0, force offset commands avoid the fall of the collective, *trim position* follows the measured positions at the *FRP* until one of the buttons' bit selectors is true. The position-dependent gravity profile of the lever at the *FRP* is inverted in sign and filtered with a discrete time first order low pass filter with rise time of 1 second. The filtering of the anti-gravity force commands is necessary for the stability of the axis. Anti-gravity force commands are necessary only when either *FTR* or *PTR* are pressed, since the spring doesn't act and the lever can't remain still in the anchor position.

The total force feedback is given by the sum of the preloaded spring action, if active, and by damping and friction factors, which are constant and are set directly in CLS units from the CLS drive model.
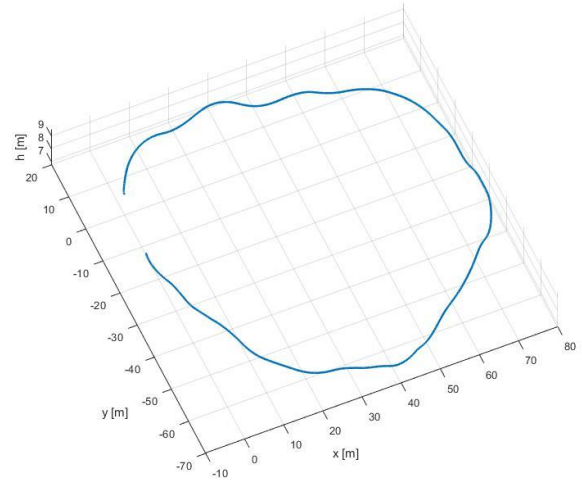
If *TB_up* is pressed, *trim position* grows at a rate of 5mm/s and consequently the lever is raised at constant speed, *TB_down* has the opposite effect. The trim velocity command is multiplied by the sampling time *Ts* so that it results in a position command. The Out of Detent *OoD* condition is true if the difference between the lever position and the commanded trim position is greater than 2mm. *OoD* should be false while the TB is pressed, but if an external force does not allow the lever to follow the trim position, the latter is forced to remain constant.

The initial trim position is passed to the ReDSim's XV-15 aircraft model for the first 2 seconds of the simulation time. After the initialization phase, the pilot can take control of the collective lever and the measured position is passed to the aircraft model.

Before the start of the simulation, a MATLAB initialization file defines the model's sampling time, the look-up tables' breakpoints for gravity compensation and measurement units' transformation, the S-function parameters of force profile and axis travel for the selected profile and the initial anchor point. *starting trim* is equal to the lower limit position of the axis travel if the simulation starts from the ground or to a position in between the limits if the simulation starts on the fly.

Figure 26. CLS drive Simulink model

Figure 17. *set trim position* subsystem

PILOT-IN-THE-LOOP SIMULATION

The CLS hardware implementation of the collective control in the ReDSim simulator with the XV-15 model is tested with pilot-in-the-loop simulations. In particular, vertical maneuvers and pirouettes are executed according to the performance standards of reference [14]. Although the maneuvers executed by the pilot can't satisfy the ADS-33E-PRF requirements for military rotorcraft, this should not be

due to CLS drive model deficiencies, but should be mainly due to the visual distortions that comes from the pilot's visual in the cockpit of the simulator, which is the one of a fixed-wing aircraft. The pilot has rated the collective's implementation according to the Cooper Harper handling qualities rating scale in reference [15] for each maneuver. A rate of 6 is given when the pirouette maneuver is executed either against the spring action or with the FRT pressed, since extensive pilot compensation is needed to meet the task requirements. A rate of 4 is given for the vertical maneuver, as the lack some visual references in the simulator has significant impact on maneuvers' execution precisions. 3-D plots of the aircraft translational motion in terms of height, lateral and longitudinal position are showed in Figures 18,19,20,21 for a vertical maneuver, a pirouette and a circuit respectively. The measured pilot force is compared to the ideal one, which is computed as the sum of the force contributions of the Control Loading Solution's estimated parameters. The comparison starts from the breakout force, as shown in Figure 22. Considering the workload of the application, a medium absolute force feedback error of 0.5N and a maximum error of 2N is satisfactory.
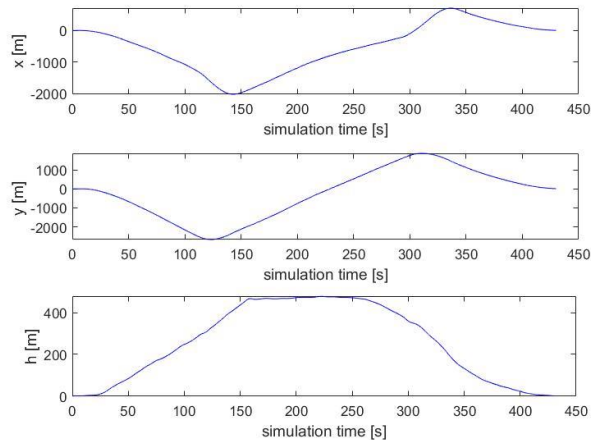

Figure 19. 3D plot of the aircraft motion during a pirouette

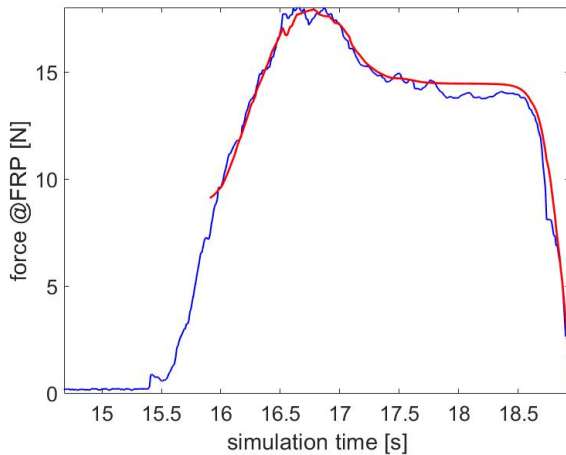**Figure 18. 3D plot of the aircraft motion during a vertical maneuver**
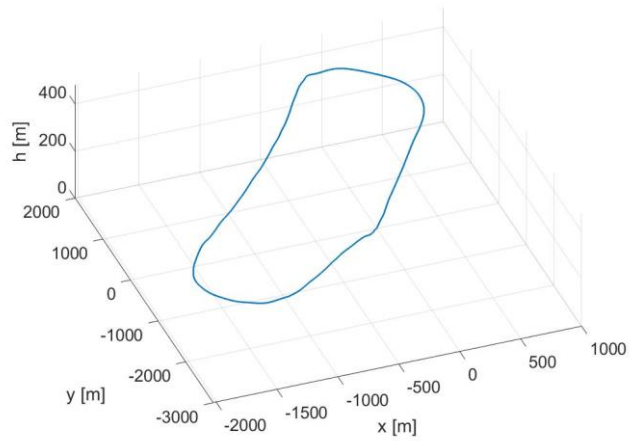
Figure 20. 3D plot of the aircraft motion during a circuit execution

8

Figure 21. Lateral, longitudinal and height variables of the aircraft motion during a circuit execution

Figure 22. Pilot applied force at the *FRP* (blue) and reference force feedback at the *FRP* (red) extracted from a simulation

CONCLUDING REMARKS

In this work, the design of a of a Control Loading Solution for a rotary wing flight simulator is presented. The drive model implements the functionalities of a tiltrotor's collective control unit and it's integrated with the aircraft's model of the simulator, which is the tiltrotor XV-15. The CLS drive model parameters are estimated by means of the classical LS estimator and a set-membership approach based on convex-relaxation of polynomial optimization problems. The Control Loading Solution hardware's motor control parameters are set from the interface software in order to reach adequate performance of force feedback release, trim input tracking and axis stability. The fidelity of the Control Loading Solution force feedback to a model of reference is performed in the time domain with pilot-in-the-loop simulation in the flight simulator of ZHAW. Although the maneuvers executed by the pilot can't satisfy the ADS-33E-PRF requirements for military rotorcraft without substantial pilot's compensation, the implementation doesn't show any major deficiency in terms of implemented functionalities and workload fidelity.

The authors are with the Dipartimento di Ingegneria Meccanica e Aerospaziale (DIMEAS), Politecnico di Torino, corso Duca degli Abruzzi 24, 10129 Torino, Italy; e-mail: *marco_rinaldi@polito.it*, *giorgio.guglieri@polito.it* and with the Zentrum für Aviatik (ZAV), Zürich Hochschule für Angewandte Wissenschaften (ZHAW), Gertrudstrasse 15, 8400 Winterthur, Switzerland; e-mail: *pierluigi.capone@zhaw.ch*

REFERENCES

[1] M. Bugaj. "The Basic Analysis of Control Systems on Commercial Aircraft". In: Perner's Contacts 6.4 (Dec. 2011), pp. 29–35. url: https://pernerscontacts.upce.cz/index.php/perner/article/view/894.

[2] A. Kuppusamy, D. Lode, "A Literature Review on Control Loading System for Aircraft Simulator", Advances in Dynamical Systems and Applications (ADSA), Vol. 16, N. 2, pp. 547-557, 2021.

[3] Jinshuo Hu, Hongbin Gu, "Survey on Flight Control Technology for Large-Scale Helicopter", International Journal of Aerospace Engineering, pp. 1-14, 2017.

[4] Z. Shutao, H. Qitao, C. Dacheng, H. Junwei, "Experiment and Study of Control Loading System in a Flight Simulator Based on RCP", IEEE International Conference on Integration Technology, Shenzhen, China, 2007.

[5] J. Zhao, G. Shen, W. Zhu, C. Yang, J. Yao, "Robust force control with a feed-forward inverse model controller for electro-hydraulic control loading systems of flight simulators", Mechatronics, Vol. 38, pp. 42-53, 2016.

[6] F. Barra, P. Capone, R. Monstein, S. Godio, G.Guglieri, "Implementation of a comprehensive mathematical model for tilt-rotor real-time flight simulation", 45th European Rotorcraft Forum, Warsaw, Poland, 17-20, September 2019.

[7] A. Abà, F. Barra, P. Capone, G. Guglieri, "Mathematical Modelling of Gimballed Tilt-Rotors for Real-Time Flight Simulation", Aerospace, Vol. 7, 2020.

[8] F. Mendoza-Mondragón, V.M. Hernández-Guzmán, R.V. Carrillo-Serrano, "Velocity regulation in PMSMs using standard Field Oriented Control plus adaptation", Asian Journal of Control, Vol. 17, N. 6, 2015.

[9] A. So, W.L. Chan, "Comprehensive model of linear PMSM-based ropeless lift for comparing control algorithms – Field-oriented control versus direct torque control", Building Services Engineering Research and Technology, Vol. 21, N. 6, 2020.

[10] Y. Kiran, P.S. Puttaswamy, "Field Oriented Control of a Permanent Magnet Synchronous Motor using a DSP", International Journal of Advanced Research, Vol. 3, N. 10, 2014.

[11] K.J. Astrom, T. Hagglund , "Advanced PID Control", ISA, 2006.

[12] Steven J. Miller, "The Method of Least Squares", The Probability Lifesaver, Princeton University Press, 2017.

[13] V. Cerone, D. Piga, D. Regruto, "Set-membership Error-In-Variables Identification Through Convex Relaxation Techniques", IEEE Transactions on Automatic Control, Vol 57, N. 2, pp. 517-522, 2012.

[14] Robert P. Harper Jr, George Emery Cooper "Handling Qualities and Pilot Evaluation", 1984 Wright Brothers Lectureship in Aeronautics, AIAA, 1984.

[15] anon., "Aeronautical Design Standard-33E-PRF, Performance Specification, Handling Qualities Requirements for Military Rotorcraft", US Army AMCOM, Redstone, Alabama, March 21, 2000.